

Relating Diffusion Tensor MRI-Derived Alterations in Myocardial Microstructure to Reduced Wall Motion in Hypertensive Left Ventricular Hypertrophy

Archontis Giannakidis¹, Alexander I Veress², Mustafa Janabi¹, James P O'Neil¹, Osama M Abdullah³, Edward W Hsu³, and Grant T Gullberg^{1,4}

¹Radiotracer Development and Imaging Technology, Lawrence Berkeley National Laboratory, Berkeley, California, United States, ²Department of Mechanical Engineering, University of Washington, Seattle, Washington, United States, ³Bioengineering, University of Utah, Salt Lake City, Utah, United States, ⁴Radiology, University of California San Francisco, San Francisco, California, United States

1. Introduction: Left ventricular hypertrophy (LVH) induced by systemic hypertension is generally regarded [1] as a morphological precursor of forthcoming unfortunate cardiovascular events. The morphological alterations that take place in hypertensive LVH (HLVH) have a direct bearing on the ventricular wall mechanics. Diffusion tensor magnetic resonance imaging (DT-MRI) [2] has emerged as a powerful tool that calculates the microstructural remodeling associated with certain cardiac diseases in a much less laborious and invasive fashion than light microscopy. Regarding cardiac mechanical function, the myocardial 1st principal strain (1-PS) is a measure that has been shown [3] to have diagnostic capability. In this work, we examine if DT-MRI is capable of detecting changes in the cardiomyocyte compartment due to HLVH. Another topic under investigation is whether myocardial 1-PS, assessed by nuclear medicine, is a sensitive cardiac index to the mechanical dysfunction that characterizes subjects with HLVH. We test the hypothesis that cardiac microstructure and function bear a reciprocal relation.

2. Materials and Methods: Animal Model and Preparation for Ex Vivo DT-MRI: We performed studies in two hearts taken from a spontaneously hypertensive rat (SHR) and an age-matched normotensive Wistar Kyoto (WKY) rat. SHR is [4] a reliable experimental model for studying essential hypertension in humans. At 22 months of age, by which time the SHR was at an advanced stage of HLVH, we removed the intact hearts from the chest, weighed and placed them in 10% formalin for fixation. The myocardial mass normalized to the body weight was 0.39% for the WKY and 0.86% for the SHR confirming the presence of LVH in the SHR, as opposed to the WKY rat. DT-MRI: Scans of the whole hearts were carried out by using a Bruker BioSpec 7T horizontal bore MRI scanner. The optimized scheme of 12 gradient directions [5] was used. The imaging parameters were: A 3D spin echo sequence, $T_R/T_E = 500/19.224$ ms, matrix size = 97×97 , resolution = 0.160mm (isotropic), nominal b -value = 1000s/mm². Regions of Interest (ROIs) - Data Analysis: We analyzed the inferolateral wall of short-axis slices covering the heart from base to apex. Maps of fractional anisotropy (FA), longitudinal (λ_L) and transverse (λ_T) diffusivities and helix angles (HA) were computed. Inter-voxel fiber regularity was quantified by using a scatter matrix-based tool called inter-voxel direction coherence index (IVDC) [6]. Streamline fiber tracking [10] was also conducted. 1-PS Computation: For the rats of this study, the myocardial 1-PS was computed at regular time points that spanned their lifetime. To acquire the deformation data, we first injected the rats with 1-1.5 mCi of ¹⁸F-fluorodihydrorotetolol (¹⁸FDHROL). Next, microPET images of the rats were obtained using the microPET/CT Inveon scanner (Siemens). The data were reconstructed into 8 separate gates of 3D images. Imaging data were semi-automatically segmented to define epi- and endocardial surfaces. Finite element (FE) models (~3000 elements) were created using geometries defined by this segmentation. The models were given realistic material properties and fiber distributions based upon the literature. Warping analysis of the end-systole and end-diastole imaging datasets was made by using Hyperelastic Warping, an FE-based image registration analysis package. For each time point, the 1-PSs were averaged over the entire LV model. Statistical Analysis: To test the statistical significance of the measured parameter differences between the control and diseased hearts, the nonparametric Mann-Whitney test was employed.

3. Results and Discussion: Qualitative fiber tracking results are shown in Fig. 1. that reveal the presence of extensive fiber disarray in the lateral wall of the SHR, as opposed to the WKY rat. The DT-MRI results are summarized in Table 1. SHR exhibited decreased FA and λ_L and increased λ_T values, when compared with the WKY. These results are consistent with the cardiomyocyte hypertrophy that is present in HLVH. In addition, the SHR demonstrated decreased IVDC values, when compared with WKY, reflecting the loss of myocardial fiber organization. Regarding the distribution of helix angles, the classic counterclockwise epicardial-to-endocardial rotation of the cardiac muscle fibers was preserved in HLVH. However, the diseased animal exhibited increased (at least triple) number of longitudinal fibers ($|HA| \geq 45^\circ$). This more oblique orientation of the cardiac muscle fibers in HLVH is attributed partly to the observed disarray and partly to the fact that in order for the muscle fibers to meet the increased contractile force demand per unit wall thickness, they start contraction from an over-stretched state. All the above DT-MRI results are in agreement with results obtained [4] three decades ago using painstaking light microscopy. The hypothesis test results indicate that the difference in all DT-MRI-derived parameters between SHR and WKY is considered to be of extreme statistical significance ($p < 0.0001$). Regarding function, the 1-PS plots for the two animals are illustrated in Fig. 2. It can be seen there that the average 1-PS for each LV were comparable for the first two time points. However, the difference in strain was found statistically significant by the third time point and thereafter ($p < 0.001$) indicating a difference in function between the SHR and WKY rats. The increased attenuation in the LV 1-PS plot in the diseased animal, over the normal case, was attributed to the progression of HLVH.

Table 1. Zonal statistical analysis of the DT-MRI parameters. FA, λ_L , λ_T and IVDC are represented by mean \pm std. The figures of longitudinal fibers ($|HA| \geq 45^\circ$) are expressed as percentages. λ_L and λ_T were normalized to the mean diffusivity. Also given are the obtained p -values by applying the nonparametric Mann-Whitney test.

	Basal area			Mid-ventricle area			Apical area		
	Control	Diseased	p -value	Control	Diseased	p -value	Control	Diseased	p -value
FA	0.3494 \pm 0.0823	0.2404 \pm 0.1174	< 0.0001	0.3324 \pm 0.0742	0.2607 \pm 0.1185	< 0.0001	0.2946 \pm 0.0710	0.2773 \pm 0.1206	< 0.0001
λ_L (10^{-5} cm ² /s)	1.3964 \pm 0.1023	1.2383 \pm 0.1269	< 0.0001	1.3698 \pm 0.0991	1.2641 \pm 0.1437	< 0.0001	1.3360 \pm 0.0902	1.2935 \pm 0.1431	< 0.0001
λ_T (10^{-5} cm ² /s)	0.8018 \pm 0.0511	0.8809 \pm 0.0635	< 0.0001	0.8151 \pm 0.0496	0.8680 \pm 0.0719	< 0.0001	0.8320 \pm 0.0451	0.8532 \pm 0.0716	< 0.0001
IVDC	0.9601 \pm 0.0235	0.8560 \pm 0.1210	< 0.0001	0.9441 \pm 0.0570	0.8358 \pm 0.1437	< 0.0001	0.9622 \pm 0.0184	0.8960 \pm 0.1327	< 0.0145
$ HA \geq 45^\circ$ (%)	13.8	55.1	-	19.8	55.6	-	18.8	73.8	-

4. Conclusions: DT-MRI allows a unique insight into the microstructural alterations after HLVH. Myocardial 1-PS was shown to have potential clinical value in assessing the mechanical impairment. The revealed changes in the cardiomyocyte compartment together with other factors (such as myocardial scarring, fibrotic stiffening, and changes in myocardial energy metabolism) play a role in modulating the mechanical properties of the myocardium in hypertensive LVH. The results in this work improve our understanding of the structural remodeling mechanisms that are associated with cardiac disorder. As well as in health, cardiac function and fiber microstructure go together also in disease. Analysis of more and younger rat hearts is in progress.

References: [1] Gradman AH et al. *Prog Cardiovasc Dis* 2006;48:326. [2] Basser PJ et al. *Biophys J* 1994;66:259. [3] Hankiewicz JH et al. *Am J Physiol Heart Circ Physiol* 2007;294:H330. [4] Kawamura K et al. *Jpn Circ J* 1976;40:1119. [5] Papadakis NG et al. *J Magn Reson* 1999;137:67. [6] Wang J et al. *Magn Reson Med* 2008;59:764.

Acknowledgements: NIH:R01 EB007219, the Director, Office of Sci, Office of Biol Environ Res, Med Sci Div, U.S. DOE under Contract DE-AC02-05CH11231.

Fig. 1 Fiber tracking results at the ROI: Control (left) and diseased (right).

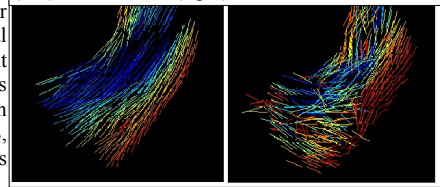


Fig. 2 Plots of the 1st principal strain of the control (left) and the diseased (right) animals.

